



Title	Classification accuracy of pain intensity induced by leg blood flow restriction during walking using machine learning based on electroencephalography
Author(s)	Imai, Hirotatsu; Kanie, Yuya; Yoshimoto, Shusuke et al.
Citation	Scientific Reports. 2025, 15, p. 27955
Version Type	VoR
URL	https://hdl.handle.net/11094/103255
rights	This article is licensed under a Creative Commons Attribution-NonCommercial-NoDerivatives 4.0 International License.
Note	

The University of Osaka Institutional Knowledge Archive : OUKA

<https://ir.library.osaka-u.ac.jp/>

The University of Osaka



OPEN

Classification accuracy of pain intensity induced by leg blood flow restriction during walking using machine learning based on electroencephalography

Hirotatsu Imai^{1,2}, Yuya Kanie^{1,2,3}✉, Shusuke Yoshimoto^{2,4}, Natsuki Yamamoto^{1,2}, Masayuki Furuya¹, Takahito Fujimori¹ & Seiji Okada¹

Pain assessment in clinical practice largely relies on patient-reported subjectivity. Although previous studies using fMRI and EEG have attempted objective pain evaluation, their focus has been limited to resting conditions. This study aimed to classify pain levels during movement using a wearable device with three forehead electrodes and advanced machine learning. Twenty-five healthy participants performed walking tasks under tourniquet-induced pain. It was confirmed that pain increased as walking time extended. Walking time was used as an index of pain stimulus intensity, and EEG data were collected to classify pain levels. Three machine learning algorithms—Random Forest, eXtreme Gradient Boosting (XGBoost), and Light Gradient Boosting Machine—were employed. XGBoost achieved the highest classification performance among them. Classification accuracy for 2-, 3-, and 5-class classifications was evaluated and compared with and without BrainRate (BR), a metric indicating changes in the frequency spectrum and reflecting relative shifts across all frequency bands. Without BR, accuracies were 0.82 for 2-class, 0.60 for 3-class, and 0.40 for 5-class classification. Including BR improved accuracies to 0.96, 0.75, and 0.47, respectively. These findings highlight the significant role of BR in improving pain classification accuracy and the potential of this system for objective pain assessment even during movement.

Keywords Electroencephalography, Artificial intelligence, Movement-related pain, Tourniquet pain, Leg blood flow restriction, Frequency spectrum

Pain is an essential signal that alerts the body to potential injury or dysfunction, serving a protective role. However, when pain becomes persistent, it can shift from a protective response to a debilitating condition. Persistent pain, particularly chronic musculoskeletal pain, significantly reduces quality of life (QOL) and impairs activities of daily living (ADL). According to the World Health Organization (WHO), chronic musculoskeletal pain is widespread, affecting 27.5% of the global population¹. Chronic musculoskeletal pain not only adversely influences health and QOL but also imposes a considerable strain on healthcare systems and the global economy. According to another report, musculoskeletal disorders contributed substantially to the global disease burden in 2017, with an estimated 1.3 billion prevalent cases, 121,300 deaths, and 138.7 million disability-adjusted life years (DALYs) worldwide². A large number of people suffer from musculoskeletal pain, whose widespread prevalence has led to increased healthcare costs, reduced workforce productivity, and a growing societal burden³.

Current pain assessment methods, such as the Visual Analogue Scale (VAS) and the Numerical Rating Scale (NRS), depend on patients' subjective self-reports⁴. This dependence can result in inconsistencies in reported pain levels and communication gaps between patients and healthcare providers. Consequently, the need for objective, automated pain assessment methods has been increasingly recognized in recent years.

¹Department of Orthopedic Surgery, Graduate School of Medicine, Osaka University, 2-2 Yamadaoka, Suita 565-0871, Osaka, Japan. ²Life-omics Research Division, Institute for Open and Transdisciplinary Research Initiative, Osaka University, Suita, Osaka, Japan. ³Health and Counseling Center, Osaka University, Toyonaka, Osaka, Japan. ⁴The Institute of Scientific and Industrial Research, Osaka University, Ibaraki, Osaka, Japan. ✉email: ykanie@ort.med.osaka-u.ac.jp

Early efforts in automatic pain assessment focused on facial expression analysis, as exemplified by Prkachin, who proposed a structured method for decoding pain intensity from facial muscle activity⁵. Subsequent studies expanded to include physiological signals such as heart rate variability, skin conductance, and pupil diameter. For instance, Treister et al. demonstrated that combining multiple autonomic parameters improved the differentiation of heat pain intensities compared to using single modalities⁶.

With advances in wearable sensors and computational power, EEG-based methods have gained prominence. Studies have shown that brain activity, particularly oscillatory dynamics, reliably encodes both noxious stimulus intensity and perceived pain intensity^{7,8}. Kächele et al. introduced a person-centered approach using physiological channels, such as ECG and EMG, for continuous pain intensity estimation, paving the way for individualized pain modeling⁹.

More recently, artificial intelligence (AI) and deep learning have enabled new possibilities for pain decoding. Wu et al. and Van Den Berg et al. leveraged deep neural networks to capture spatial-spectral-temporal EEG patterns for real-time pain assessment^{10,11}. Transformer-based models have also been explored, such as the work by Lu et al., which employed multiscale deep learning for physiological signal-based pain classification¹². Furthermore, multimodal approaches integrating EEG with surface EMG have been proposed to improve classification performance in chronic pain contexts, as shown by De et al.¹³.

Despite these advances, few studies have addressed the challenge of assessing pain during movement—a scenario frequently encountered in real-world and clinical settings. Many existing studies rely on experimental pain models under resting conditions, which limit their applicability to daily life or postoperative pain.

In this study, we introduced the HARU-2, a novel patch-type EEG, and utilized a wireless communication system for EEG signal collection in an attempt to detect and identify pain during movement. This device is lightweight, comfortable to wear, equipped with stretchable, flexible electrodes, and features high-precision analog circuitry, enabling the accurate measurement of EEG signals of $1\mu\text{V}$ or less¹⁴. This sensor is designed to be worn on the frontal region of the subject's head, where there is minimal contact with hair. It provides reliable EEG signals with lower noise levels than those obtained from frontopolar electrodes of conventional EEG systems (Fpz, Fp1, and Fp2). These advances in EEG measurement technology, combined with AI-based analysis methods, have opened up new possibilities for assessing pain-related neural activity during movement. The aim of this study is to evaluate the classification accuracy (Acc) of wearable EEG combined with AI analysis in identifying the presence and intensity of pain during movement.

Materials and methods

Participants

In this experiment, 25 healthy subjects (22 males and 3 females, aged 33.2 ± 2.0 years) participated. The inclusion criteria required that participants report no pain at the time of the experiment, were not taking any medication (including analgesics), and had no history of developmental delays or cognitive impairments. All participants received a detailed explanation of this experimental protocol, which was approved by the Institutional Review Board of Osaka University Hospital (No. 22187). All research procedures were conducted in accordance with the relevant guidelines and regulations, including the Declaration of Helsinki. Written informed consent was obtained from all participants prior to their participation.

Experimental pain modalities

The tourniquet-induced pain model was used as the experimental pain stimulus, which was evoked by restricting leg blood flow during walking. While it has been reported that pain intensity from tourniquet application increases over time¹⁵, we conducted the following experiment to investigate whether this feature persists during walking. Each participant walked with an air tourniquet wrapped around both lower legs. To minimize noise during walking, participants were instructed to limit head and neck movements as much as possible during EEG measurements and to maintain a steady pace of 80 steps per minute. The walking task was performed on an indoor track approximately 15 m in circumference. Initially, they walked for 2 min at a tourniquet pressure of 0 mmHg (Task 0). Subsequently, they continued walking while the tourniquet pressure was increased and maintained at 200 to 250 mmHg to induce sufficient lower extremity ischemia. Painful walking was performed for a total of 8 min, divided into four 2-minute segments labeled as Tasks 1 through 4. Tourniquet pressure was checked after each task and adjusted to remain within the specified range (Fig. 1).

Pain rating

Pain intensity for each task was assessed using the NRS immediately after the completion of each task. The NRS ranges from 0 (no pain) to 10 (the worst imaginable pain).

Electroencephalography recording

Brain activity was recorded using a patch-type EEG device (HARU2; PGV, Tokyo, Japan) with three electrodes placed on the forehead (L: left, Z: center, R: right) and a reference electrode positioned on the mastoid behind the left ear. This device employs low-noise electrode materials¹⁶, and both the electrodes and electrode base are flexible, allowing for a secure and comfortable fit to the forehead. In addition, the wired connection between the electrodes and the EEG unit is minimized, and wireless signal transmission helps to reduce motion artifacts. EEG signals were sampled at 250 Hz. EEG data from the last minute of each 2-minute task's second half (Tasks 0–4) were analyzed and labeled as EEG0–4.

Machine learning was employed to evaluate the Acc of classifying pain levels during movement. Three different classification approaches were performed. In the first scheme, 'No Pain' and 'Worst Pain' classes were compared to determine whether brainwaves could determine the presence or absence of pain in participants. The second approach involved a three-level classification ('No Pain', 'Medium Pain', and 'Worst Pain') to assess

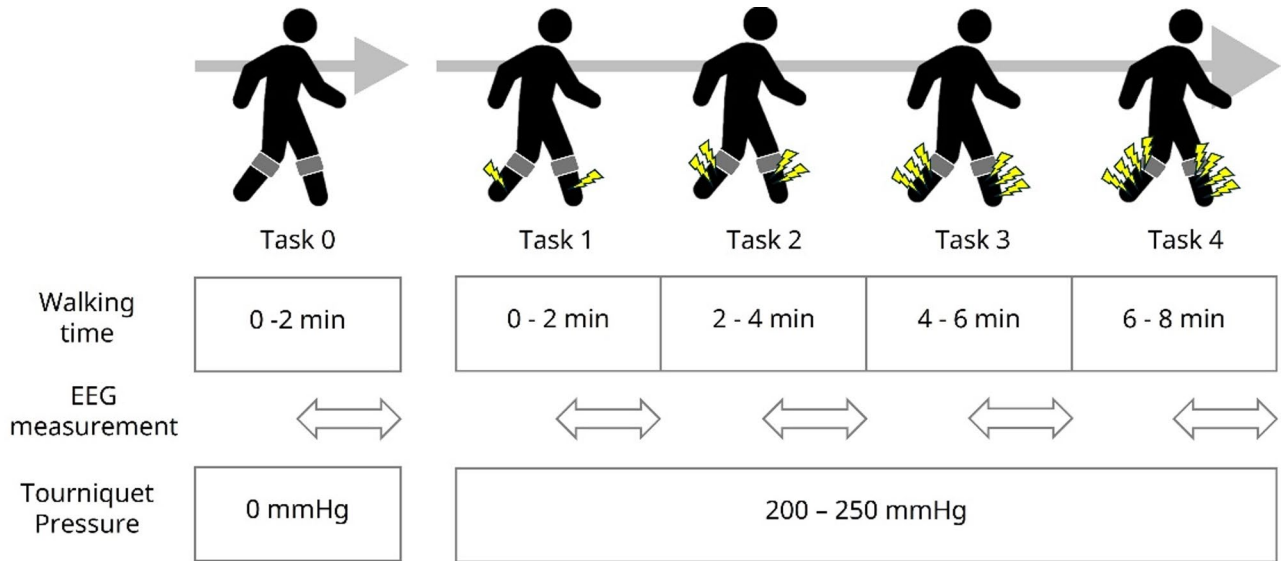


Fig. 1. Experimental Protocol of EEG measurements. Participants walked with air tourniquets wrapped around both lower legs. They first walked for 2 min with the tourniquet pressure set to 0 mmHg (Task 0). Afterward, they continued walking as the tourniquet pressure was gradually increased and maintained between 200 and 250 mmHg. They walked under these painful conditions for a total of 8 min, divided into four 2-minute segments (Tasks 1–4). The tourniquet pressure was checked after each segment and adjusted as needed to stay within the specified range. EEG recorded during the last minute of each task was analyzed.

Classification	Descriptive classes	Corresponding EEG data
2-class classification	No Pain, Worst Pain	EEG0, EEG4
3-class classification	No Pain, Medium Pain, Worst Pain	EEG0, EEG2, EEG4
5-class classification	No Pain, Mild Pain, Medium Pain, Severe Pain, Worst Pain	EEG0, EEG1, EEG2, EEG3, EEG4

Table 1. Definition of classification schemes and class labels. This table outlines the three classification tasks and defines the descriptive class names used in the analysis, along with their corresponding source EEG data recorded during each experimental task.

whether pain levels could be classified into distinct stages. The third approach aimed for a more detailed classification, dividing pain levels into five categories ('No Pain', 'Mild Pain', 'Medium Pain', 'Severe Pain', and 'Worst Pain'). A summary of the examined classification schemes is provided in Table 1.

Electroencephalography preprocessing

Filtering process

EEG preprocessing involved applying a band-pass filter (0.5–90 Hz) and a blink artifact filter using wavelet transformation¹⁷. Additionally, a threshold filter (400 μ V) was applied to remove motion artifacts.

Frequency analysis

Cleaned EEG data were segmented into 2-second epochs using a Hamming window with 50% overlap. For each epoch, the frequency power spectrum was calculated using Fast Fourier Transform (FFT) for the following bands: Theta (4–8 Hz), Alpha (8–13 Hz, including Low Alpha [8–10 Hz], Middle Alpha [10–12 Hz], and High Alpha [12–13 Hz]), Beta (13–26 Hz, including Low Beta [13–18 Hz] and High Beta [18–26 Hz]), and Gamma (26–90 Hz).

A metric called BrainRate (BR)¹⁸ was also calculated. BR reflects the spectral center of gravity and indicates relative changes across the entire frequency band. BR was computed using the following Eq. (1):

$$\text{BrainRate (BR)} = \frac{\sum_{i=1}^L (freq_i * power_i)}{\sum_{i=1}^L power_i} \quad (1)$$

In this formula, $freq_i$ denotes the center frequency of the i -th frequency bin, and $power_i$ represents the spectral power at that frequency. L is the total number of bins spanning the 0.5–90 Hz frequency range. This measure provides a compact representation of the frequency distribution of EEG signals, where higher BrainRate

values indicate dominance of higher frequency activity, and lower values indicate stronger presence of lower frequencies.

Furthermore, the obtained feature values were standardized using Z-score normalization to correct individual differences. Each feature x_i was centered in Eq. (2):

$$x_{iz} = \frac{x_i - x_{mean}}{x_{std}} \quad (2)$$

Here, x_{mean} and x_{std} represent the mean and standard deviation of the features used for each subject and each task, respectively. For example, in the case of 3-class classification, EEG0, EEG2, and EEG4 are used; therefore, x_{mean} and x_{std} are calculated as the mean and standard deviation of the features from EEG0, EEG2, and EEG4 for each subject. This centering process accounts for individual differences and facilitates comparisons across datasets. For each subject and task, the 1-second frequency power spectra obtained through the windowing process were summed and averaged to derive the feature values.

Data analysis and statistics

A subject-wise 5-fold cross-validation was used to evaluate the model's performance. The participants were divided into five distinct groups: one group served as the test set, and the remaining four were used as the training set in each iteration. This process was repeated five times, ensuring that each group was used as the test dataset once. The performance metrics obtained from the five iterations were averaged to determine the final performance metrics of the model. Three machine learning algorithms—Random Forest (RF), eXtreme Gradient Boosting (XGBoost), and Light Gradient Boosting Machine (LightGBM)—were evaluated in this process. These three algorithms were selected because they are applied using the same preprocessing methods. This approach eliminates bias due to differences in preprocessing and ensures a fair comparison across the models. The algorithm with the highest classification accuracy was selected as the final model. Classification performance was evaluated using a confusion matrix, including the following Eqs. (3)–(5):

$$Accuracy (Acc) = \frac{TP + TN}{TP + FN + TN + FP} \quad (3)$$

$$Precision = \frac{TP}{TP + FP} \quad (4)$$

$$Recall = \frac{TP}{TP + FN} \quad (5)$$

TP, TN, FP, and FN represent true positives, true negatives, false positives, and false negatives, respectively.

Statistical analysis

All data were analyzed using IBM SPSS statistics version 27.0 (IBM Corp., Armonk, NY), and are presented as means \pm SDs. Statistical analyses were performed using one-way analysis of variance (ANOVA) to evaluate differences among groups. For post-hoc multiple comparisons, the Bonferroni correction was applied to identify significant differences between groups. A significance level of $p < 0.05$ was considered statistically significant.

Results

Pain rating

Participants' self-reported pain intensity on the NRS were as follows; mean values for each task were 0 ± 0 for task 0, 4.2 ± 1.0 for task 1, 6.2 ± 1.1 for task 2, 7.8 ± 0.9 for task 3, and 9.0 ± 0.8 for task 4, which showed that their perception of pain increased over time (Fig. 2). Significant differences were observed between tasks ($p < 0.05$). These findings suggest that walking time could serve as an objective indicator of pain.

Frequency power spectrum

Figure 3 shows the frequency power spectra of preprocessed EEG data from a representative subject. Each graph represents the theta, alpha, beta, and gamma bands during a series of walking tasks extracted from three channels (ChZ, ChR, and ChL). Vertical dashed lines indicate task transitions.

Comparison of algorithms and model selection

The performance results of the three algorithms (RF, XGBoost, and LightGBM) are presented in Table 2. All performance metrics are reported as classification accuracy. While some algorithms occasionally matched or exceeded XGBoost's accuracy for specific classes, XGBoost consistently delivered the highest overall performance and was therefore selected as the final model for this study.

Classification using frequency power spectrum

The results of the three types of classification using XGBoost are presented in Fig. 4. The figure presents the Acc of each classifier, with values of $Acc = 0.82$ for the 2-class classification, $Acc = 0.60$ for the 3-class classification, and $Acc = 0.40$ for the 5-class classification. Additionally, the figure shows the confusion matrix and provides the precision for each classification.

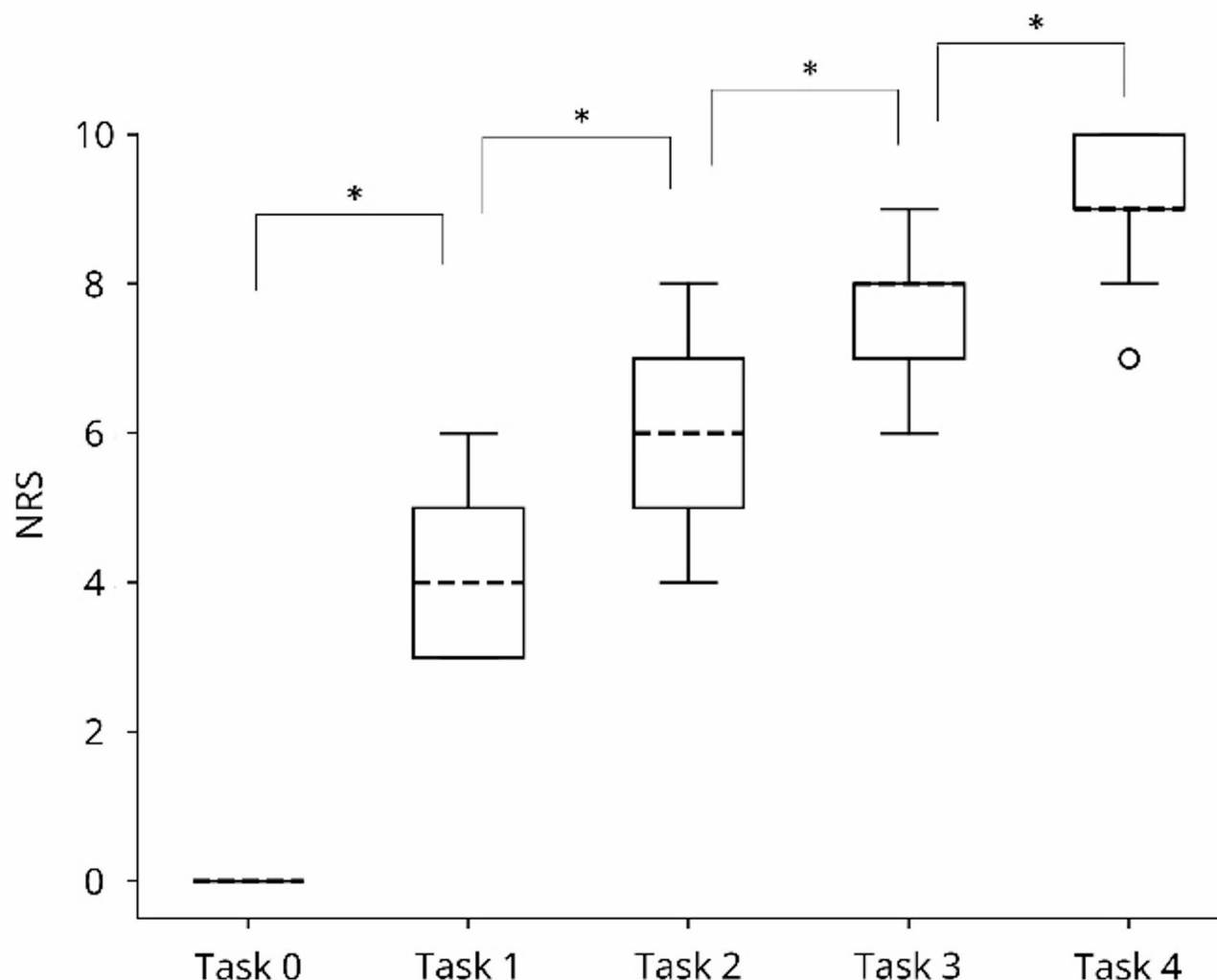


Fig. 2. Boxplots of NRS, an indicator of pain intensity during walking, across the five tasks. The self-reported pain intensity increased over time, with significant differences observed between each task ($p < 0.05$).

Classification using frequency power spectrum with BR

The results of the three classifications using XGBoost, when power spectrum with BR was included, are presented in Fig. 5. The figure presents Acc of each classifier, with values of $Acc = 0.96$ for the 2-class classification, $Acc = 0.75$ for the 3-class classification, and $Acc = 0.47$ for the 5-class classification. Additionally, the figure shows the confusion matrix and provides the precision for each classification.

Discussion

This study is the first to report the use of leg blood flow restriction during walking as a model for quantitatively applying pain stimuli during movement. According to Pyati et al., intra-neuronal ischemia is the underlying mechanism of tourniquet-induced pain¹⁹. They also reported that prolonged tourniquet application increases the risk of intra-neuronal ischemia, with pain intensifying as the duration extends. In this study, it was demonstrated that pain associated with walking under tourniquet compression increased over time. This finding confirmed its utility as progressively increasing pain during movement. Pain intensity was categorized into five levels based on walking duration, and machine learning was applied to classify these levels. The classification Acc varied significantly depending on whether BR, which represents the center of gravity of the frequency spectrum, was included in the training data. BR contributed substantially to 2-class and 3-class classification, but in 5-class classification, performance did not significantly exceed the baseline accuracy (ChanceRate), even when BR was included.

Various instruments have been used to objectively assess pain. In a fMRI study, Wager, T. D. et al. investigated the neural signature elicited by thermal pain stimuli, identifying key brain regions such as the thalamus, posterior and anterior insula, secondary somatosensory cortex, anterior cingulate cortex, and central gray matter. The authors concluded that fMRI could be utilized to analyze brain activity patterns and objectively measure pain intensity without relying on self-reports. However, these techniques have certain limitations. Firstly, MRI

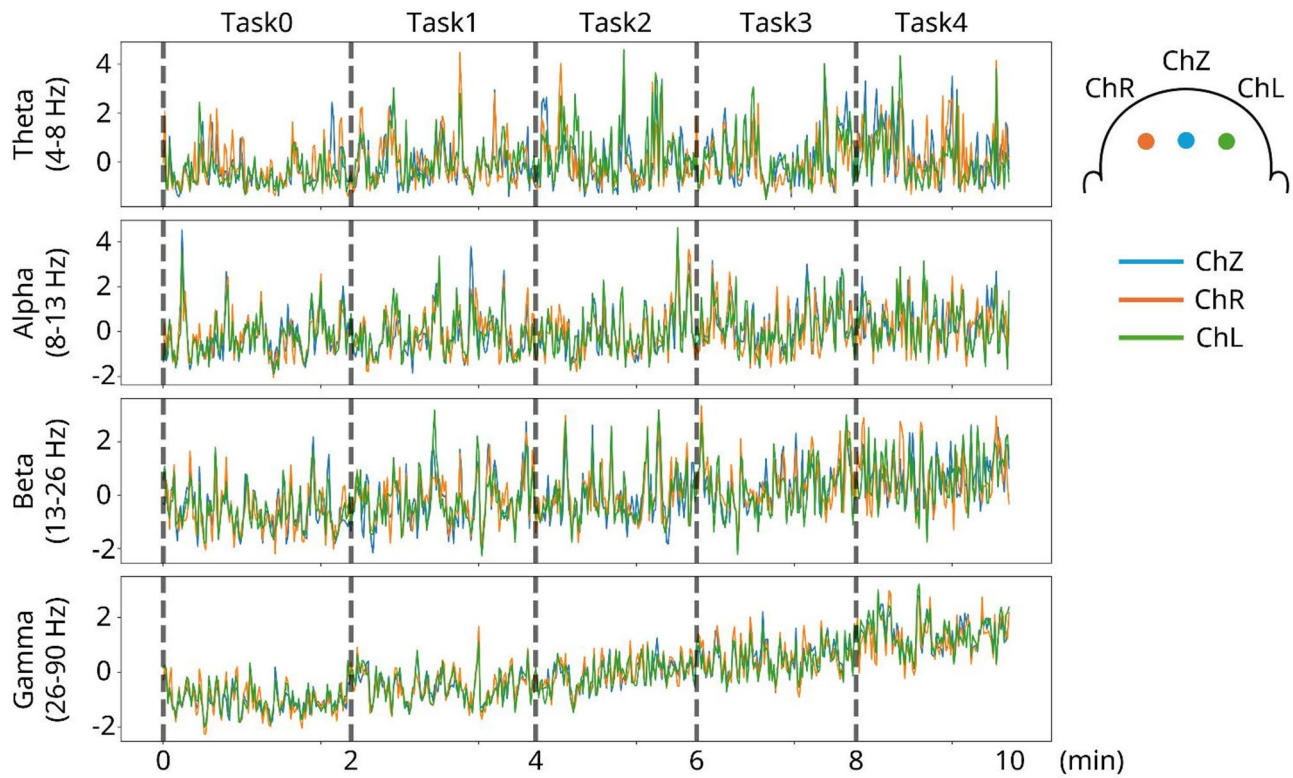


Fig. 3. Frequency power spectra of the preprocessed EEG signal. The graph shows standardized features in the theta (4–8 Hz), alpha (8–13 Hz), beta (13–26 Hz), and gamma (26–90 Hz) frequency bands extracted from three EEG channels (ChZ, ChR, and ChL) during the walking task. The horizontal axis represents time, and the vertical axis represents the standardized values of each frequency band ($x_{iz} = (x_i - x_{mean})/x_{std}$). Vertical dashed lines indicate the transition between tasks (task 0 to task 4).

		RF	XGBoost	Light GBM
2-class	Without BR	0.70	0.82	0.78
	With BR	0.86	0.96	0.88
3-class	Without BR	0.46	0.60	0.64
	With BR	0.56	0.75	0.78
5-class	Without BR	0.32	0.40	0.27
	With BR	0.33	0.47	0.38

Table 2. Performance comparison of algorithms (Acc). The performance of three algorithms (RF, XGBoost, and LightGBM) was compared for each classification task (2-class, 3-class, and 5-class). Each task was analyzed both with and without using BR as a feature. The performance values are the final model metrics, which were averaged from a subject-wise 5-fold cross-validation. While some algorithms occasionally matched or exceeded XGBoost's accuracy for specific classes, XGBoost consistently delivered the highest overall performance and was therefore selected as the final model for this study. All values represent classification accuracy (Acc).

systems are expensive and require large equipment, making them impractical for installation in smaller medical facilities. Secondly, they can only measure pain under controlled conditions, restricting their use for assessing pain in daily life.

In contrast, electroencephalography (EEG) is the most commonly used modality due to its affordability and non-invasive nature. However, traditional multi-electrode EEG systems with long wires also have limited applicability, as they are generally confined to specific environments. In recent years, several studies have utilized AI to classify pain objectively using EEG signals. For example, Nezam et al. used a 30-electrode EEG system to classify cold-induced pain into three or five levels, achieving 83% accuracy for three-level and 60% for five-level classification²⁰. Similarly, Modares-Haghghi et al. employed 29 electrodes and reported 92% accuracy for binary classification and 86% for five-level pain classification²¹. Wu et al. developed a model that learned spatial-spectral-temporal features from EEG signals for subject-independent pain estimation¹⁰, while Van Den Berg et

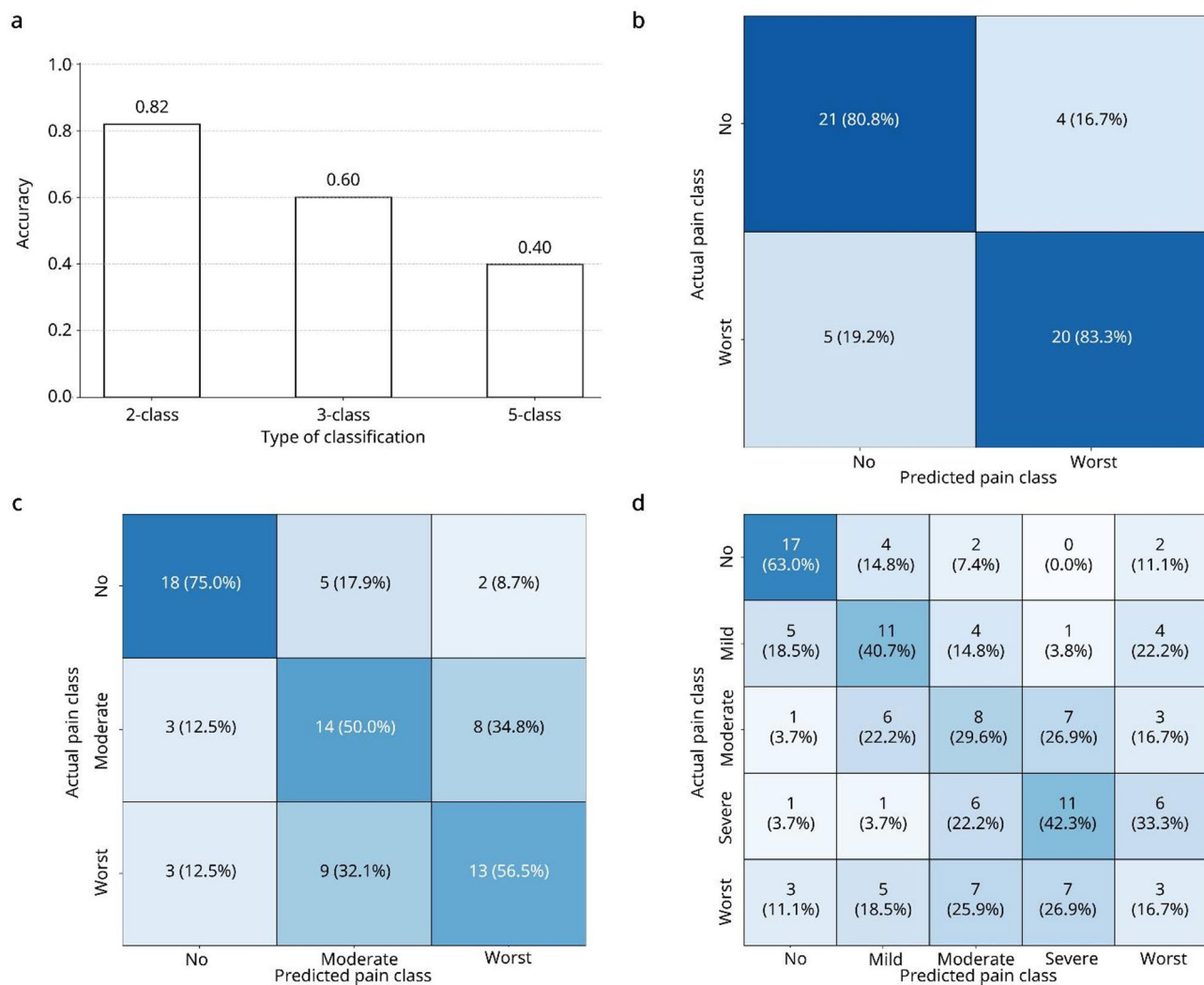


Fig. 4. Evaluation of three types of classifications using XGBoost with frequency power spectrum as the training data. **(a)** Comparison of accuracy (Acc) for each class classification. **(b – d)** Confusion matrix for 2-class, 3-class, and 5-class classification. The matrix shows the absolute counts of correctly and incorrectly classified instances, along with the precision percentages for each class.

al. estimated perceptual thresholds in real-time based on EEG without requiring participant responses¹¹. Lu et al. proposed a transformer-based model to classify pain using physiological signals¹². De et al. combined EEG with surface electromyography (sEMG) in a multimodal framework to classify chronic low back pain into four severity levels¹³.

Although these AI-based approaches have shown promising results, all of them were conducted under resting or controlled experimental conditions. To our knowledge, no previous study has evaluated pain classification during physical movement using EEG. Therefore, this study is the first to assess pain classification accuracy during movement using a compact, wearable EEG device. Our approach addressed challenges such as noise caused by the presence of cords and the loss of mobility. While our results showed lower Acc compared to previous studies conducted in the resting state, the Acc for 2-class and 3-class classifications was still high. This suggests that it is possible to objectively classify pain even under the challenging conditions of using only three frontal-region electrodes and performing measurements during movement, which is typically less favorable for EEG analysis.

In this study, the BR index, in addition to the frequency spectrum of each band, was included in the training data. For all classifications, incorporating BR significantly improved Acc compared to results obtained without it. Although there have been a few reports examining individual frequency bands^{7,22}, no studies have specifically investigated BR, which quantifies the center of gravity of the frequency spectrum. The findings of this study suggest that BR is particularly sensitive to changes during pain stimulation.

This study has several limitations. First, the sample size was small, with only prospectively collected EEG data from 25 healthy subjects. To address this limitation, we employed a five-fold cross-validation method. This approach avoided the risk of data leakage between the training and test sets by dividing the dataset into five

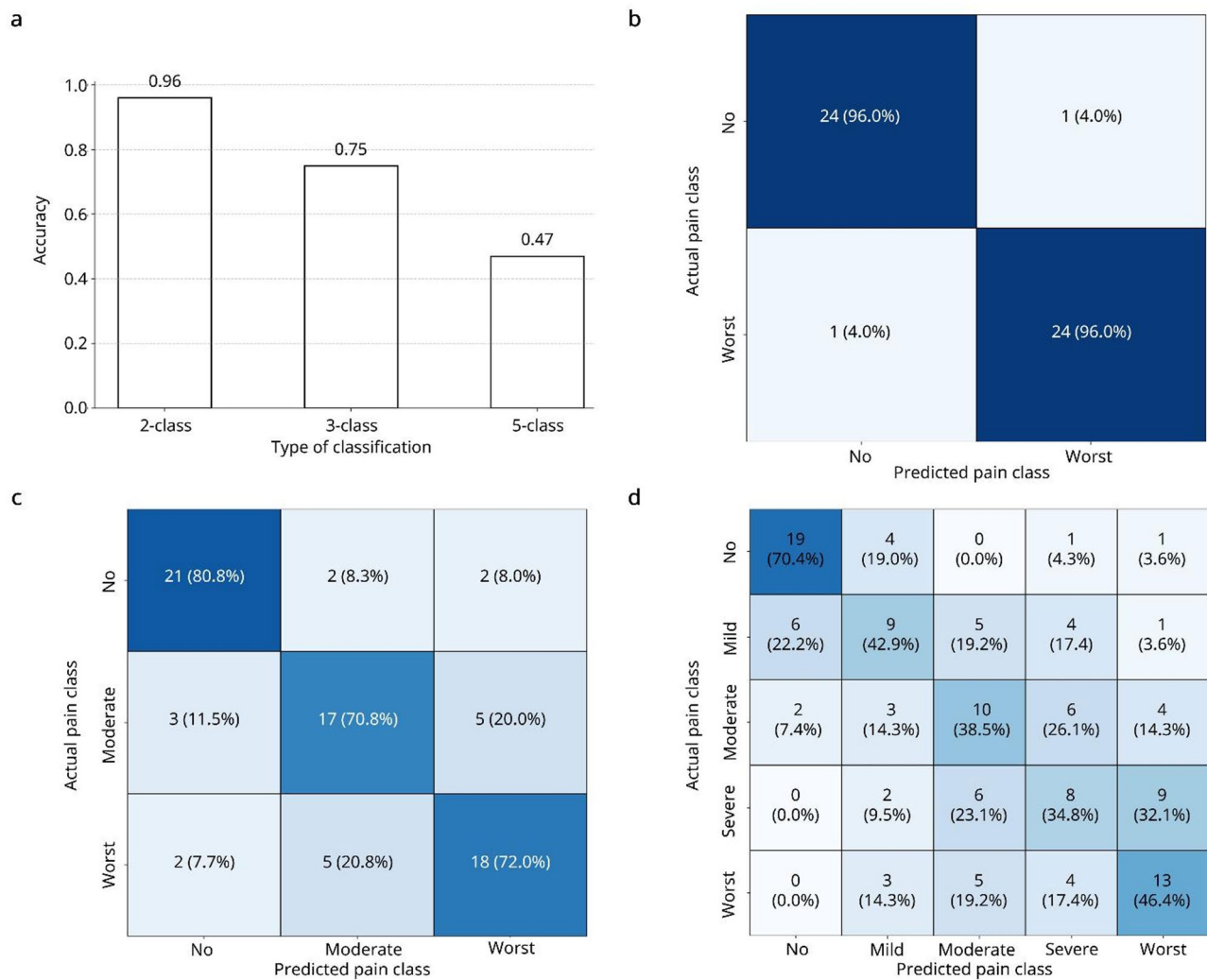


Fig. 5. Evaluation of three types of classifications using XGBoost with frequency power spectrum and BrainRate as the training data. **(a)** Comparison of accuracy (Acc) for each class classification. **(b – d)** Confusion matrix for 2-class, 3-class, and 5-class classification. The matrix shows the absolute counts of correctly and incorrectly classified instances, along with the precision percentages for each class.

separate groups and ensuring that each participant's data was assigned to only one group per fold and evaluated once as independent test data. This method was particularly suited to our limited dataset, as it allowed for reliable performance evaluation while reducing the potential for overfitting. Second, the primary focus of this study was to assess the feasibility of using a wearable EEG device to evaluate pain during movement, rather than to compare multiple machine learning models. Therefore, only three machine learning algorithms were evaluated in this study, and the optimal algorithm was selected from among them. There are, however, various other machine learning methods that could be considered. Exploring other algorithms may further enhance the robustness and versatility of the pain classification model. Finally, the level of pain perceived in response to a specific pain stimulus can vary between individuals. Even when the same level of pain is experienced, self-reported pain levels may differ due to variations in individual pain sensitivity, which is shaped by personal experiences. In the future, it will be essential to develop a more advanced system that accounts for individual differences in pain sensitivity to improve classification Acc.

Conclusion

A machine learning model was developed to objectively evaluate pain using equipment designed for real-world clinical settings. Previous research has been constrained by equipment limitations, with most studies focusing on brain activity recorded in the resting state. In contrast, our study utilized a low-noise wearable device to record brain activity and demonstrated that pain intensity can be accurately classified even during movement.

These findings suggest that EEG-based pain classification using compact and wearable sensors is feasible under dynamic conditions, opening the door to objective pain assessment in real-world environments such as rehabilitation settings and postoperative monitoring. Furthermore, the introduction of BrainRate as a spectral metric significantly improved classification accuracy, highlighting its potential as a novel biomarker for pain

intensity. Future studies with larger cohorts and diverse pain models are warranted to validate the generalizability and clinical utility of this approach.

Data availability

The datasets generated and/or analyzed during this study are available from the corresponding author upon reasonable request.

Received: 7 February 2025; Accepted: 24 July 2025

Published online: 31 July 2025

References

1. Zimmer, Z., Fraser, K., Grol-Prokopczyk, H. & Zajacova, A. A global study of pain prevalence across 52 countries: examining the role of country-level contextual factors. *Pain* **163**, 1740–1750 (2022).
2. Safiri, S. et al. Prevalence, deaths, and Disability-Adjusted life years due to musculoskeletal disorders for 195 countries and territories 1990–2017. *Arthritis Rheumatol. Hoboken NJ* **73**, 702–714 (2021).
3. Elliott, A. M., Smith, B. H., Penny, K. I. & Smith, C. Alastair chambers, W. The epidemiology of chronic pain in the community. *Lancet* **354**, 1248–1252 (1999).
4. Breivik, H. et al. Assessment of pain. *Br. J. Anaesth.* **101**, 17–24 (2008).
5. Prkachin, K. M. Assessing pain by facial expression: facial expression as nexus. *Pain Res. Manag.* **14**, 53–58 (2009).
6. Treister, R., Kliger, M., Zuckerman, G., Aryeh, I. G. & Eisenberg, E. Differentiating between heat pain intensities: the combined effect of multiple autonomic parameters. *Pain* **153**, 1807–1814 (2012).
7. Schulz, E. et al. Prefrontal gamma oscillations encode tonic pain in humans. *Cereb. Cortex N Y N* **25**, 4407–4414 (2015).
8. Nickel, M. M. et al. Brain oscillations differentially encode noxious stimulus intensity and pain intensity. *NeuroImage* **148**, 141–147 (2017).
9. Kachele, M., Thiam, P., Amirian, M., Schwenker, F. & Palm, G. Methods for Person-Centered continuous pain intensity assessment from Bio-Physiological channels. *IEEE J. Sel. Top. Signal. Process.* **10**, 854–864 (2016).
10. Wu, F. et al. Learning Spatial-Spectral-Temporal EEG representations with deep Attentive-Recurrent-Convolutional neural networks for pain intensity assessment. *Neuroscience* **481**, 144–155 (2022).
11. Van Den Berg, B., Vanwassen, L., Jansen, N. & Buiteweg, J. R. Real-time Estimation of perceptual thresholds based on the electroencephalogram using a deep neural network. *J. Neurosci. Methods.* **374**, 109580 (2022).
12. Lu, Z., Ozek, B. & Kamarthi, S. Transformer encoder with multiscale deep learning for pain classification using physiological signals. *Front. Physiol.* **14**, 1294577 (2023).
13. De, S., Mukherjee, P., Roy, A. H. & GLEAM A multimodal deep learning framework for chronic lower back pain detection using EEG and sEMG signals. *Comput. Biol. Med.* **189**, 109928 (2025).
14. Araki, T. et al. Skin-Like transparent sensor sheet for remote healthcare using electroencephalography and photoplethysmography. *Adv. Mater. Technol.* **7**, 2200362 (2022).
15. Bakri, M. H., Ismail, E. A. & Abd-Elshafy, S. K. Analgesic effect of Nalbuphine when added to intravenous regional anesthesia: A randomized control trial. *Pain Physician.* **19**, 575–581 (2016).
16. Kondo, M. et al. Ultralow-Noise organic transistors based on polymeric gate dielectrics with Self-Assembled modifiers. *ACS Appl. Mater. Interfaces* **11**, 41561–41569 (2019).
17. Islam, M. K., Rastegarnia, A., Yang, Z. A. & Wavelet-Based Artifact reduction from scalp EEG for epileptic seizure detection. *IEEE J. Biomed. Health Inf.* **20**, 1321–1332 (2016).
18. Pop-Jordanova, N. & Pop-Jordanov, J. Spectrum-weighted EEG frequency ('brain-rate') as a quantitative indicator of mental arousal. *Prilozi* **26**, 35–42 (2005).
19. Pyati, S. et al. Effects of tourniquets in the development of pain states: a novel clinical pilot study and review of utilization of tissue oximetry to measure neural ischemia. *Curr. Pain Headache Rep.* **24**, 25 (2020).
20. Nezam, T., Boostani, R., Abootalebi, V. & Rastegar, K. A novel classification strategy to distinguish five levels of pain using the EEG signal features. *IEEE Trans. Affect. Comput.* **12**, 131–140 (2021).
21. Modares-Haghghi, P., Boostani, R., Nami, M. & Sanei, S. Quantification of pain severity using EEG-based functional connectivity. *Biomed. Signal. Process. Control.* **69**, 102840 (2021).
22. Egggaard, L. L., Wang, L. & Arendt-Nielsen, L. Volunteers with high versus low alpha EEG have different pain-EEG relationship: a human experimental study. *Exp. Brain Res.* **193**, 361–369 (2009).

Acknowledgements

This study was supported by J & J Medical Research Grant (2024-2025, AS2024A000094585, Yuya Kanie), and Life-omics Interdisciplinary Research Promotion Grant (2024-2025, Hirotatsu Imai). We thank the technical staffs of PGV, Tokyo, Japan for their helpful discussions and comments.

Author contributions

H.I. drafted the initial manuscript. H.I. and Y.K. collected and analyzed the data. S.Y. contributed to data analysis and provided critical feedback. N.Y., M.F., and T.F. provided research advice. S.O. supervised the study. All authors reviewed and approved the final manuscript.

Declarations

Competing interests

The authors declare no competing interest. The funding sponsor had no role in the design of the study; collection, analyses, or interpretation of data; writing of the manuscript; or decision to publish the results.

Additional information

Correspondence and requests for materials should be addressed to Y.K.

Reprints and permissions information is available at www.nature.com/reprints.

Publisher's note Springer Nature remains neutral with regard to jurisdictional claims in published maps and institutional affiliations.

Open Access This article is licensed under a Creative Commons Attribution-NonCommercial-NoDerivatives 4.0 International License, which permits any non-commercial use, sharing, distribution and reproduction in any medium or format, as long as you give appropriate credit to the original author(s) and the source, provide a link to the Creative Commons licence, and indicate if you modified the licensed material. You do not have permission under this licence to share adapted material derived from this article or parts of it. The images or other third party material in this article are included in the article's Creative Commons licence, unless indicated otherwise in a credit line to the material. If material is not included in the article's Creative Commons licence and your intended use is not permitted by statutory regulation or exceeds the permitted use, you will need to obtain permission directly from the copyright holder. To view a copy of this licence, visit <http://creativecommons.org/licenses/by-nc-nd/4.0/>.

© The Author(s) 2025